"soft armor" regulates the electrocatalytic microenvironment for

nitrate reduction to ammonia to greatly enhance stability

Experiment section

Chemicals

The titanium mesh (1 mm thick) was purchased from Kangwei Department (Dalian, China). Anhydrous sodium sulfate (Na_2SO_4), ferric chloride hexahydrate ($FeCl_3 \cdot 6H_2O$), polyacrylamide (PAM), N,N-dimethylacrylamide, ammonium persulfate (APS), tetramethylethylenediamine ($C_6H_{16}N_2$), ammonium sulfate 14N (($^{14}NH_4)_2SO_4$, 98.5%), ammonium sulfate ^{15}N (($^{15}NH_4)_2SO_4$, $\geq$ 99 at%, 98.5%), sodium nitrate ^{14}N ($Na^{14}NO_3$, 98.5%), sodium nitrate ^{15}N ($Na^{15}NO_3$, $^{15}N \geq$ 99 at%, 98.5%), maleic acid ($C_4H_4O_4$, $\geq$ 99.0%), and deuterium oxide (D_2O, 99 at% D) were purchased from Sigma-Aldrich. Hydroxylamine hydrochloride ($NH_2HO \cdot HCl$), 1,10-phenanthroline ($C_{12}H_8N_2 \cdot HCl$), and ammonium iron(III) sulfate dodecahydrate ($NH_4Fe(SO_4)_2 \cdot 12H_2O$) were purchased from Sinopharm Chemical Reagent Co., Ltd. Milli-Q water (18.25 MΩ cm-1) was used throughout the experiments. Before use, the Ti mesh pieces were ultrasonically rinsed in acetone, ethanol, and deionized water for 15 minutes each to completely remove surface impurities and native oxides. All chemicals were used without further purification.

Synthesis of FeOOH/Ti

(1) Treat the titanium mesh sequentially in hydrochloric acid, acetone, and ethanol for appropriate durations to remove surface impurities.

(2) Place the pretreated titanium mesh flat in a mixed solution of 0.03M Na_2SO_4 and $FeCl_3 \cdot 6H_2O$ with equal concentrations. React under water bath conditions at 60°C for 12 hours to obtain the FeOOH catalyst. Different concentrations of Na_2SO_4 and $FeCl_3 \cdot 6H_2O$ are used to synthesize different FeOOH catalysts.

Preparation of PAM/FeOOH

Dissolve 0.65g of PAM, 0.06g of N,N-dimethylacrylamide, and 0.03g of APS in 10 ml of ultrapure water to obtain a mixed solution. Place the prepared FeOOH/Ti (1cm*3cm) in a mold, add 5ml of the mixed solution to the mold, then add 20ul of tetramethylethylenediamine and mix well. Allow it to stand; the polyacrylamide hydrogel will rapidly polymerize. After polymerization, dialyze the product using ultrapure water three times, each time for 10 minutes.

Preparation of P-PAM/FeOOH

During the preparation process of PAM/FeOOH, after adding 20ul of tetramethylethylenediamine and mixing well, the mold is placed into liquid nitrogen 10 seconds later. Once the mixed solution solidifies, it is removed and left to thaw at room temperature.

Material characterizations

Scanning electron microscopy (SEM) images were acquired using a Zeiss Supra 40 scanning electron microscope at an acceleration voltage of 5 kV. Transmission electron microscopy (TEM) images were recorded using a JEOL JEM-2010-TEM with an accelerating 70 voltage of 200 kV. The powder X-ray diffraction (XRD) pattern was obtained using a Philips X'Pert PRO SUPER X-ray diffractometer equipped with graphite-monochromated Cu Kα radiation (λ = 1.54056 Å). X-ray photoelectron spectroscopy (XPS) measurement was performed on an X-ray photoelectron 75 spectrometer (ESCALab MKII). The ultraviolet-visible (UV-Vis) absorbance spectra were measured on Shimadzu UV-3900 spectrophotometer. The isotope labeling experiments were measured by ^{1}H NMR measurement (JNM-ECZ600R).

Ion concentration detection methods

The concentrations of nitrate, nitrite, and ammonium were determined using colorimetric methods.1 A ultraviolet-visible (UV-Vis) spectrophotometer was employed to detect the ion concentrations of the electrolytes after diluting them to appropriate concentrations to match the range of the calibration curves.2 The specific detection methods are as follows:

Determination of Nitrate (NO_3^--N): The nitrate concentration was measured according to standard procedures. Firstly, a certain amount of electrolyte was taken from the electrolytic cell and diluted to 5 mL to ensure it was within the detectable range. Then, 100 μL of a 5% (w/w) sulfamic acid solution was added to the solution, which was allowed to stand at room temperature for 10 minutes. The absorption spectrum was tested using a UV-Vis spectrophotometer, and the absorption intensities at wavelengths of 220 nm and 275 nm were recorded. The final absorbance value was calculated using the equation: A = A220 nm - 2A275 nm. A calibration curve was plotted using a series of solutions with concentrations ranging from 0 to 2.50 ppm. The sodium nitrate used for plotting the calibration curve was dried in an oven at 105-110°C for 2 hours beforehand.

Determination of Nitrite (NO_2^--N): A mixture of 0.4 g of p-aminobenzenesulfonamide, 0.02 g of N-(1-naphthyl)ethylenediamine dihydrochloride, 5 mL of ultrapure water, and 1 mL of phosphoric acid (ρ=1.70 g/mL) was used as the color reagent. A certain amount of electrolyte was taken from the electrolytic cell and diluted to 5 mL to ensure it was within the detectable range. Next, 0.1 mL of the color reagent was added to the aforementioned 5 mL solution and mixed uniformly. After allowing it to stand for 20 minutes, the absorption intensity at a wavelength of 540 nm was recorded. A concentration-absorbance curve was calibrated using a series of standard sodium nitrite solutions.

Detection of Ammonium (NH_4^+-N): Nessler's reagent was prepared by dissolving 0.35 g of potassium iodide (KI) and 0.5 g of mercuric iodide (HgI_2) sequentially in 5 mL of 4.0 M sodium hydroxide (NaOH) solution. The mixed solution was then allowed to stand in the dark without disturbance for 24 hours. Finally, the supernatant was transferred to a Teflon bottle and refrigerated for use. For the colorimetric assay, a certain amount of electrolyte was taken from the electrolytic cell and diluted to 5 mL to ensure it was within the detectable range. Next, 0.1 mL of a 500 g/L potassium

sodium tartrate solution was added and mixed thoroughly. Then, 0.1 mL of Nessler's reagent was added to the solution. After allowing it to stand for 20 minutes, the absorption intensity at a wavelength of 420 nm was recorded. A concentration-absorbance curve was plotted using a series of standard ammonium chloride solutions ranging from 0 to 2.50 ppm. The ammonium chloride crystals used for plotting the calibration curve were dried at 105°C for 2 hours beforehand.

Determination of Hydroxylamine(NH_2OH): The measurement of hydroxylamine concentration follows a standard procedure. Firstly, a certain amount of electrolyte is taken from the electrolytic cell and diluted to 5 milliliters to ensure it is within the detectable range. Then, 100 microliters of sodium acetate-acetic acid buffer solution (1 mol/L + 1 mol/L) with a pH of around 4.5, ammonium iron(III) sulfate solution (4.0 mmol/L), and 1,10-phenanthroline-ethanol (0.01 mol/L) solution are sequentially added to the solution, which is then allowed to stand at room temperature for color development for 30 minutes. The absorption spectrum is tested using a UV-Vis spectrophotometer, and the absorption intensity at a wavelength of 510 nanometers (corrected from 510 nm, assuming it was a typo) is recorded. A calibration curve is plotted using a series of hydroxylamine solutions with concentrations ranging from 0 to 1 ppm.

Electrochemical nitrate reduction experiment

The electrochemical nitrate reduction reaction experiment was conducted using a standard three-electrode system in a single-chamber electrolytic cell. The catalyst loaded on titanium mesh, the saturated calomel electrode (SCE), and platinum foil served as the working electrode, reference electrode, and counter electrode, respectively. A 0.5 M solution of sodium sulfate (Na_2SO_4) was used as the electrolyte, and a certain concentration of sodium nitrate ($NaNO_3$) was added to the electrolytic cell as the target reactant. All electrochemical measurements were performed using the CHI 660E electrochemical workstation from Chenhua Instruments, Shanghai. The potential was recorded relative to the standard hydrogen electrode (RHE), with the conversion formula being E(RHE) = E(SCE) + 0.0591 × pH + 0.2438. Prior to conducting the nitrate electroreduction test, a linear sweep voltammetry test was performed to stabilize the polarization curve. Subsequently, potentiostatic tests were carried out at different potentials for a duration of 2 hours.

In the amplification experiment, PAM/FeOOH with a size of 60cm * 45cm was used as the cathode. Use a DC power supply for electrolysis, with an electrolyte concentration of 0.1M Na2SO4+200ppm NO3-N, and each electrolysis experiment lasts for 6 hours.

The electrolyte concentration in the article is described as follows: the low concentration electrolyte contains 50ppm NO_3^-N from $NaNO_3$ and 0.5mol/L Na_2SO_4, while the high concentration electrolyte contains 500ppm NO_3^-N from $NaNO_3$ and 0.5mol/L Na_2SO_4.

The experiment on the adsorption of NH2OH by P-PAM

We conducted the experiment in two solutions of NH2OH with a concentration of 20 ppm. One of the solutions was placed with the prepared working electrode P-PAM/FeOOH for 60 minutes, after which a color developing agent used in the hydroxylamine test was added for color comparison.

Calculation of the Faradaic efficiency (FE) and yield rate

The FE of NH_3 and NO_2^- was calculated as follows:

$FE(NH_3)=8*F*C_{NH3}*V)/(17*1000*Q)*100\%$

$FE\ NO_2^-=(2*F*C_{NO2^-}*V)/(46*1000*Q)*100\%$

The yield rate of NH_3 and NO_2^- was calculated according to the following equation:

$Y_{NH3}=(C_{NH3}*V)/(A*t_c)$

$Y_{NO2-}=(C_{NO2-}*V)/(A*t_c)$

Where F is the Faradaic constant (96485 C mol^{-1}); CNH_3 and $C\ C_{NO2^-}$ represent the concentration of NH_3 and NO_2^- (mg L^{-1}), respectively; V is the volume of the electrolyte (L); Q is the total amount of charge (C): absolute integral value of i-t curve under "multi-potential step" mode; A is the geometric area of working electrode (cm^{-2}), tc is the NO_3^- electrolysis time on cathode (h).

N isotope labeling experiments

Using the electrochemical nitrate reduction method, nitrogen isotope labeling experiments were conducted in electrolyte solutions containing Na^{15}NO$_3$ and Na^{14}NO$_3$ as nitrogen sources, respectively, at a concentration of 50 ppm NO$_3^-$-N. The amounts of ^{15}NH$_4^+$-N and ^{14}NH$_4^+$-N produced were quantified using ^{1}H-Nuclear Magnetic Resonance (NMR) spectroscopy. For quantification, a series of standard solutions were prepared and a standard curve was plotted. Firstly, a series of ^{15}NH$_4^+$-N solutions with known concentrations were prepared in 0.5 M Na$_2$SO$_4$ as standards. Secondly, 50 mL of ^{15}NH$_4^+$-N solutions and standard solutions at different concentrations were mixed with 50 ppm maleic acid. Thirdly, 50 μL of deuterium oxide (D$_2$O) was added to the 0.5 mL mixed solution for NMR detection. Fourthly, calibration was achieved using the peak area ratio between ^{15}NH$_4^+$-N and maleic acid, as the concentration of ^{15}NH$_4^+$-N was positively correlated with the area ratio. Similarly, this method was also used to quantify the amount of ^{14}NH$_4^+$-N when Na^{14}NO$_3$ was used as the nitrogen source.

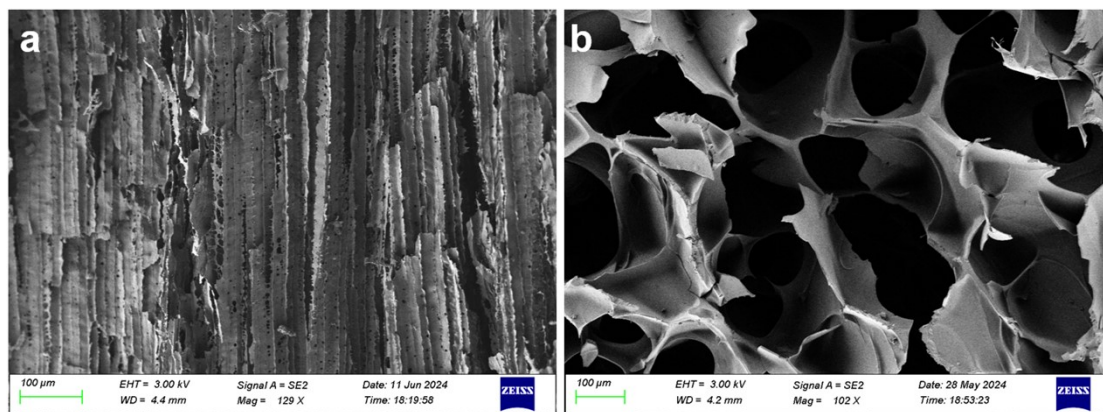**Fig. S1.** The SEM image of P-PAM synthesized by a conventional method, (a) and (b) represent longitudinal section and cross-section, respectively.
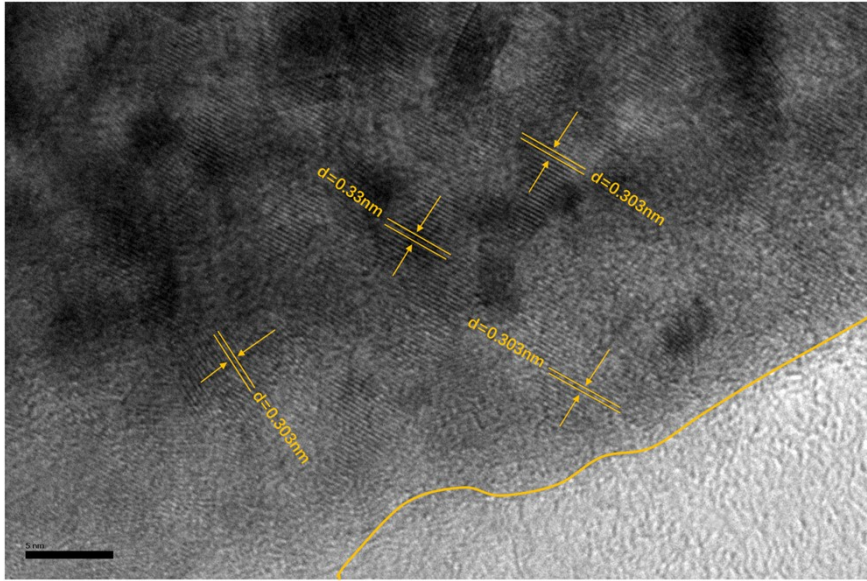
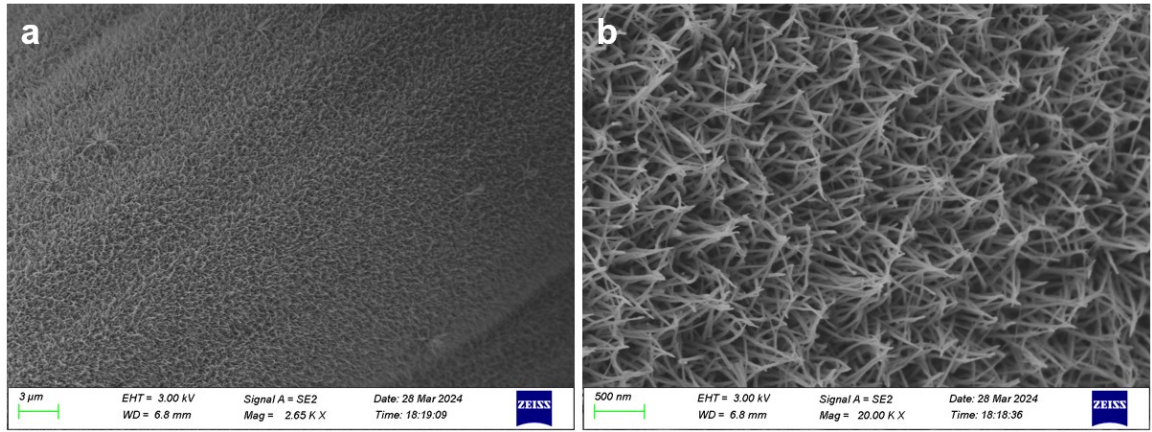**Fig. S2.** The TEM image of P-PAM/FeOOH.
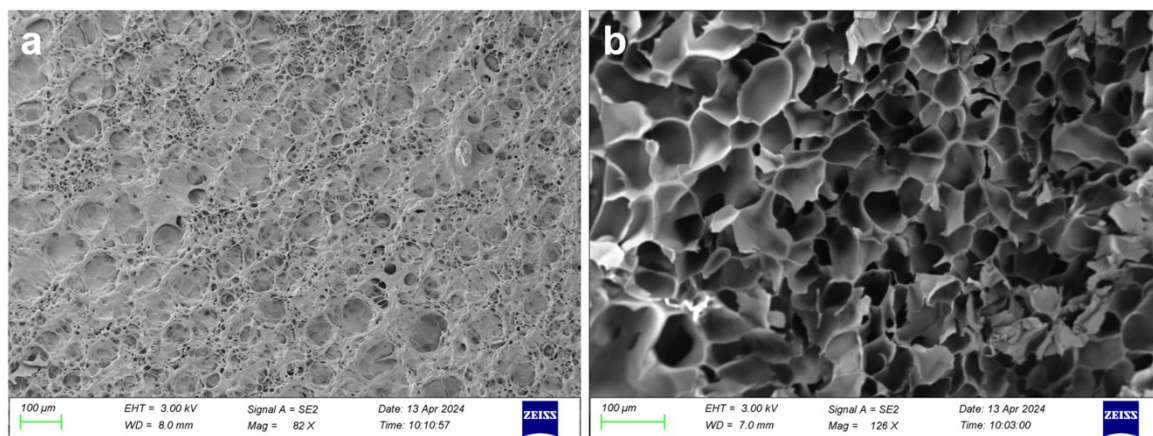
Fig. S3. The SEM image of FeOOH/Ti.

Fig. S4. The SEM image of PAM synthesized by a conventional method, (a) and (b) represent cross-section and longitudinal section, respectively.
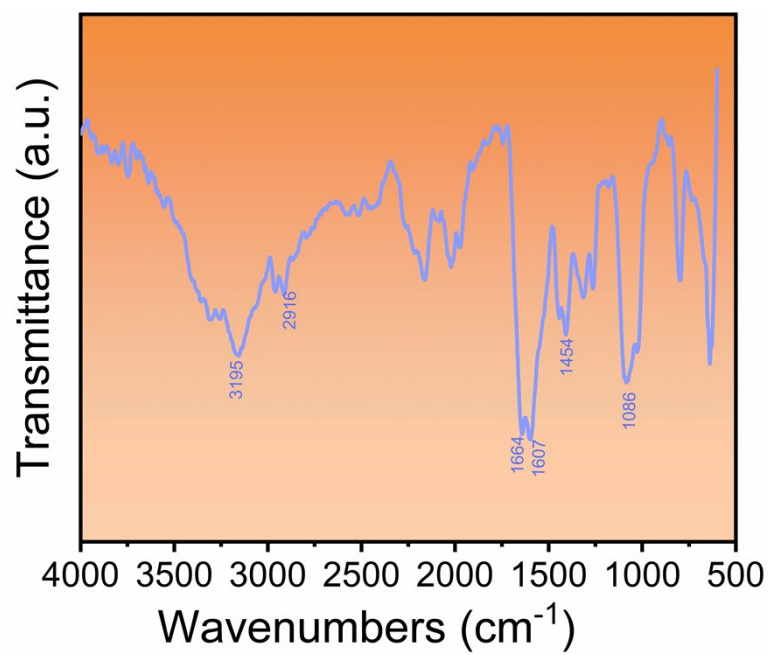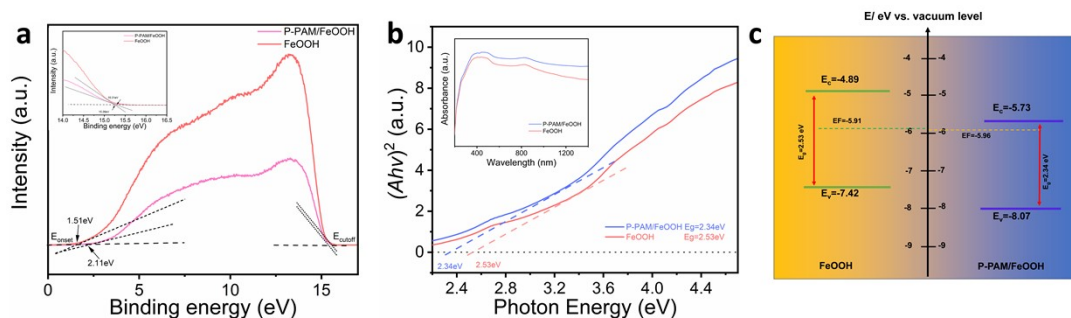
Fig. 5. FTIR spectrum of P-PAM.

Fig. S6. (a) Ultraviolet photoelectron spectroscopy (UPS) of FeOOH and P-PAM/FeOOH (the inset presents an enlarged view of the cutoff energy region for FeOOH and P-PAM/FeOOH); (b) Tauc plots derived from the UV-Vis diffuse reflectance spectra of FeOOH and P-PAM/FeOOH (the inset shows the UV-Vis diffuse reflectance spectra of FeOOH and P-PAM/FeOOH); (c) Schematic diagram of the energy band structure of FeOOH and P-PAM/FeOOH (EF: Fermi level; EC: conduction band energy; EV: valence band energy; Eg: band gap).
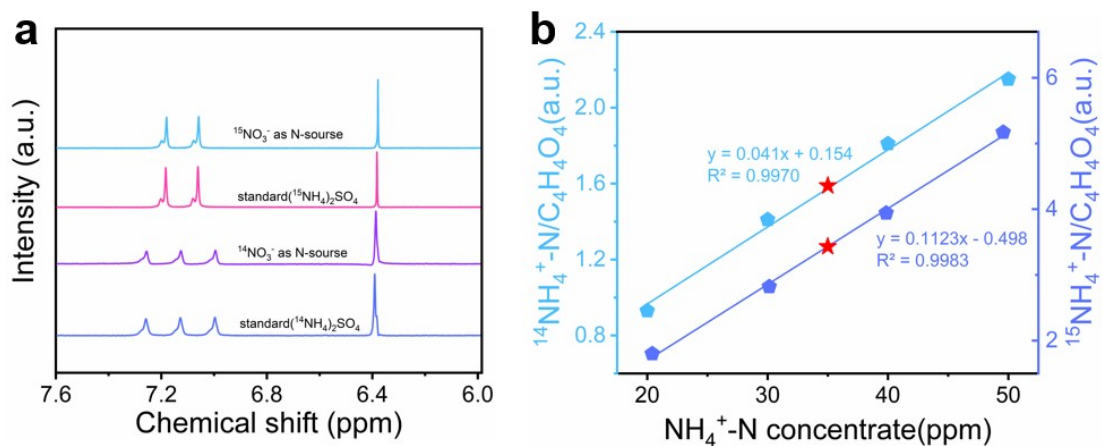
Fig. S7. (a)1H NMR spectra (600 MHz) after 2 h of reduction at -0.6 V vs. RHE using standard samples ((15NH4)2SO4 and (14NH4)2SO4), and electrolytes with 14NO3- and 15NO3- as N sources. (b)Isotope labeling method for ^{1}H NMR spectrum, standard curves of different N sources, and the ammonium concentration corresponding to this work.
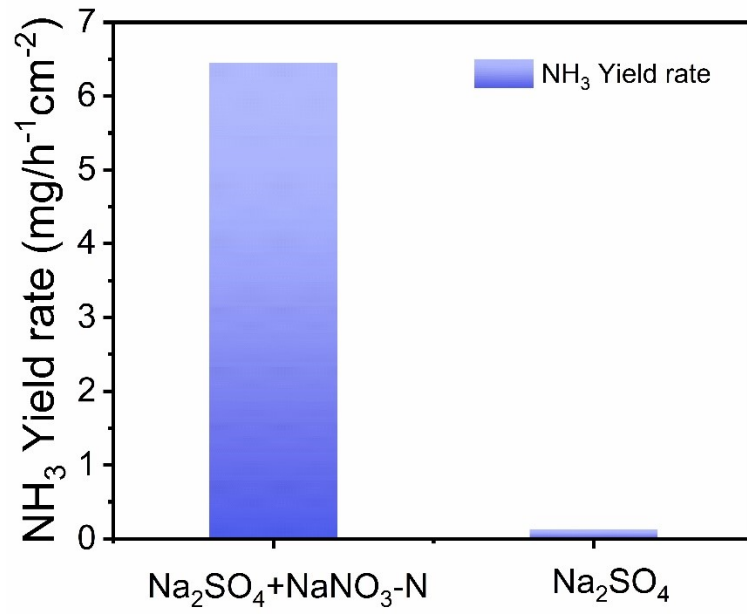
Fig. S8. Ammonia yield rate under conditions with and without nitrate.
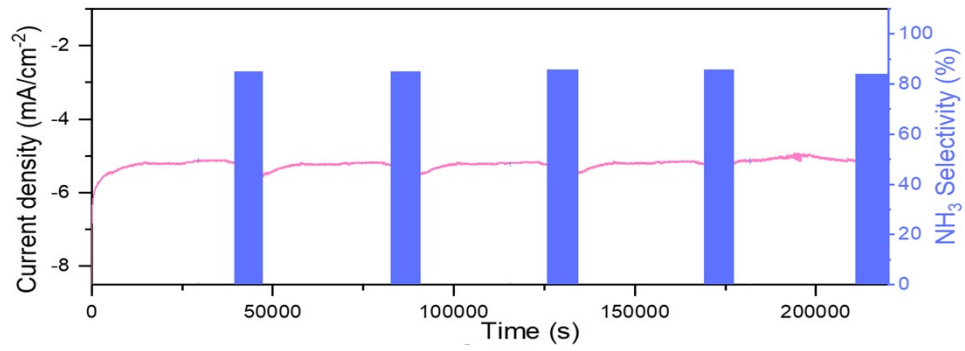
Fig. S9. Current density and NH_3 selectivity in the cyclic electrolysis experiment of P-PAM/FeOOH in 500 ppm NO_3^--N +0.01 M NaOH electrolyte solution at -0.6V.
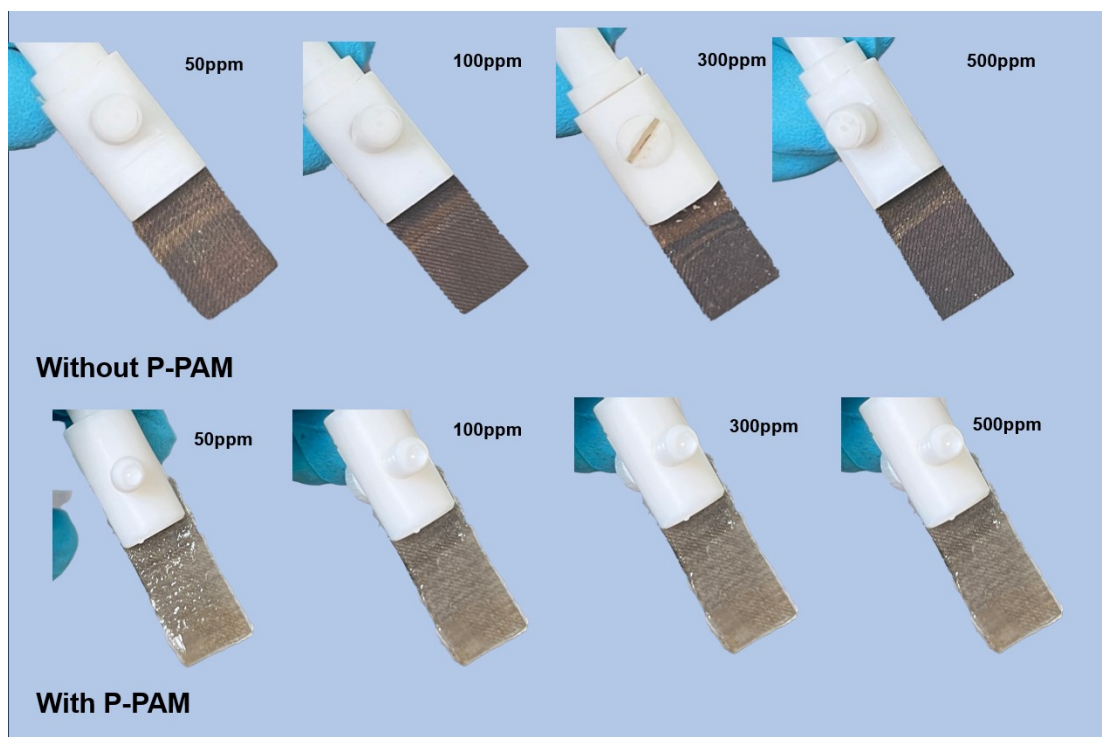
Fig. S10. Optical images of the electrodes after electrolysis experiments at different potentials in 0.5M Na_2SO_4 electrolyte solution without NO_3^--N. Optical images of the electrodes after electrolysis experiments in 0.5M Na2SO4 electrolyte solutions with different concentrations of NO_3^--N.
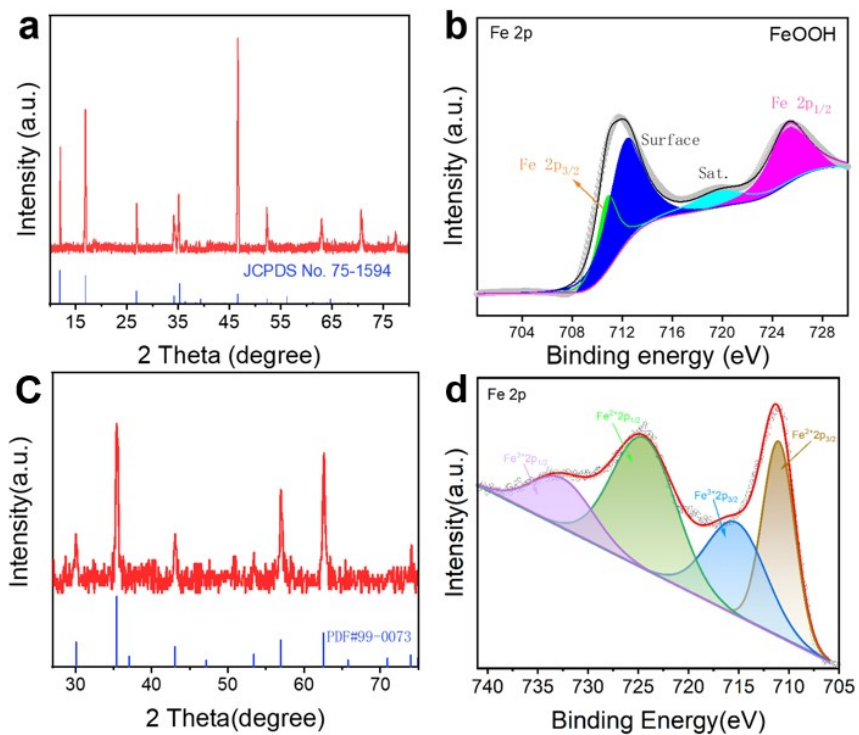
Fig. S11. (a), (b) are XRD and XPS of FeOOH before electrolysis, respectively, (c), (d) are XRD and XPS of FeOOH after electrolysis, respectively.
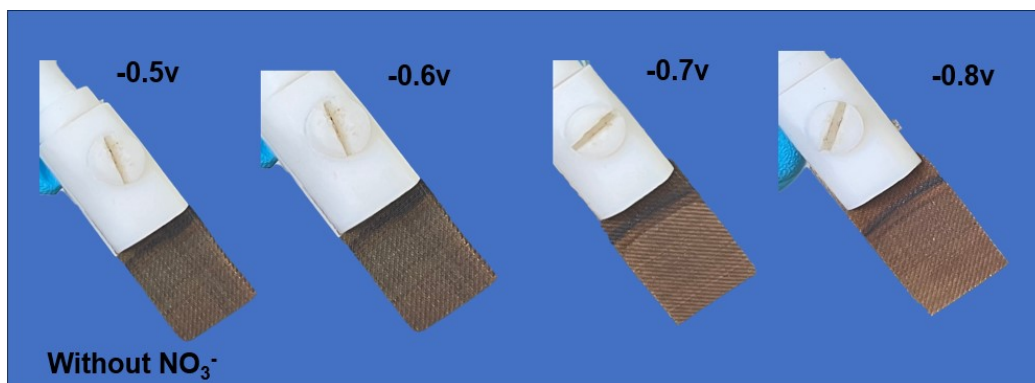
Fig. S12. Optical images of electrolysis at different potentials in 0.5 M Na$_2$SO$_4$ electrolyte.
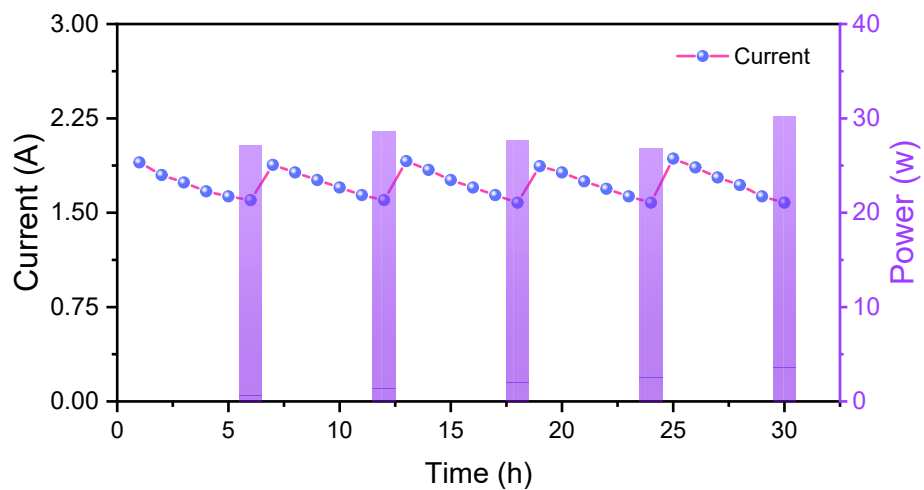
Fig. S13. Current and average power of the amplified material during cyclic experiments (6 hours per cycle).
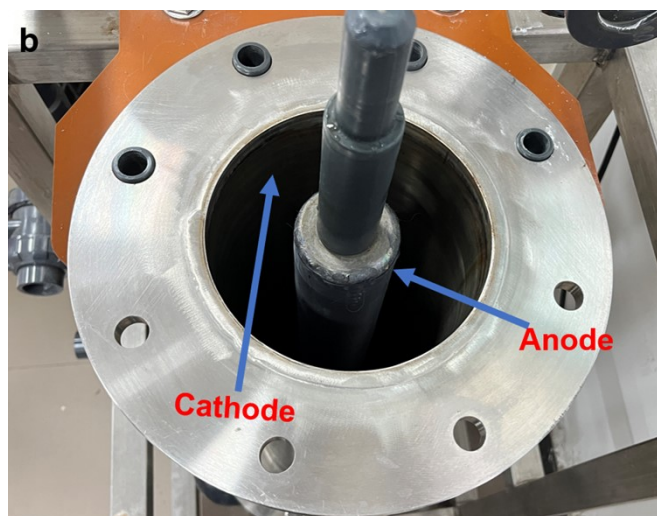
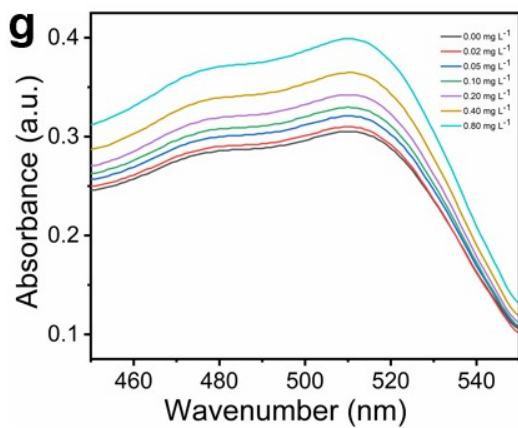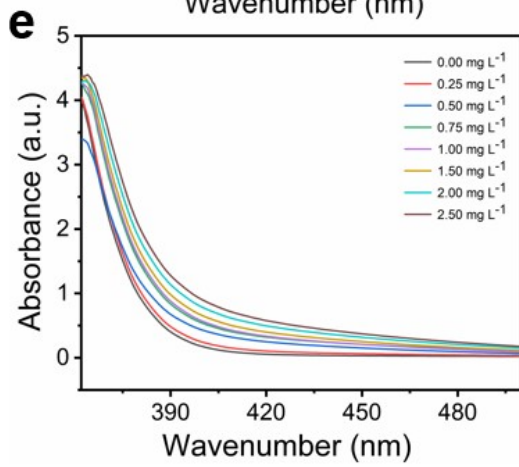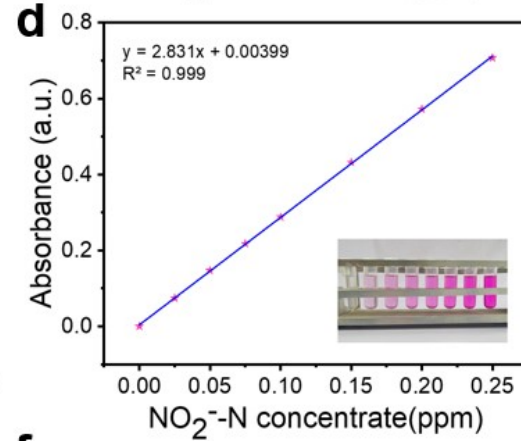**Fig. S14.** (a). Photos of the magnifying device. (b). The internal structure diagram of the device.
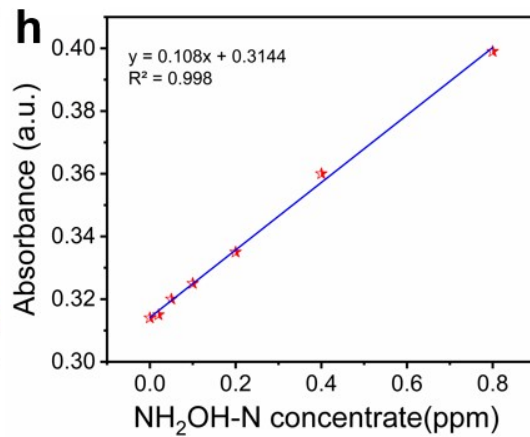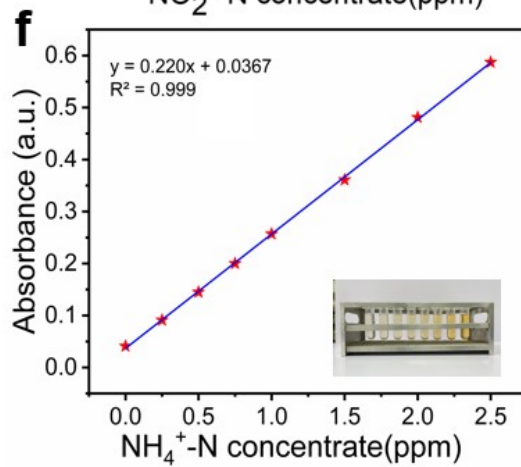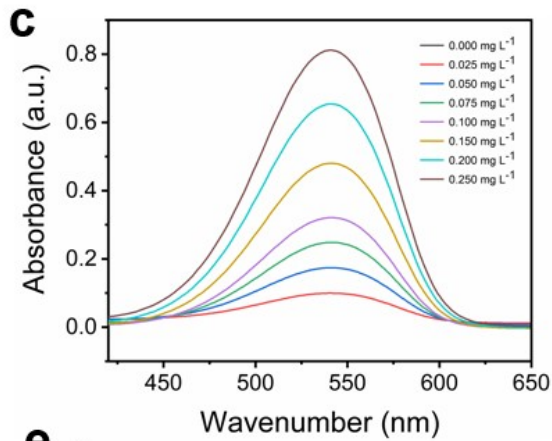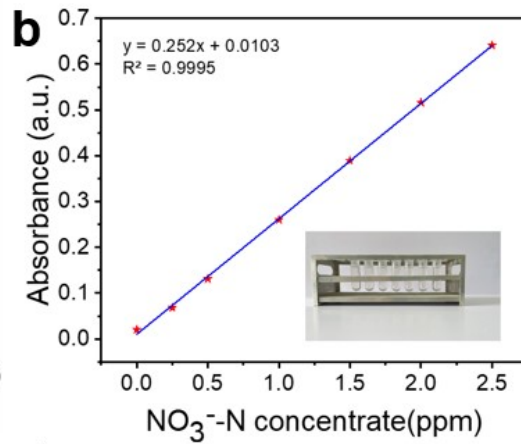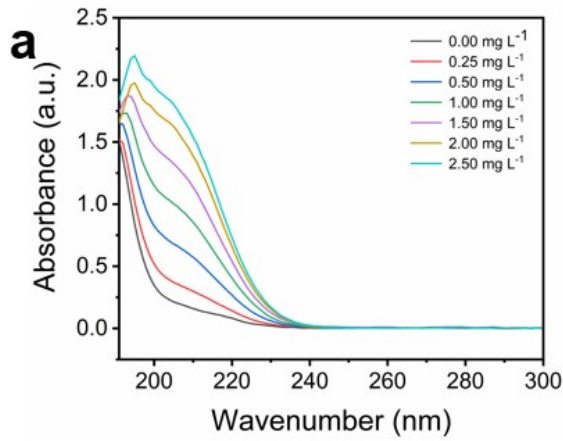
Fig. S15. (a), (c), (e) and (g) represent the concentration-absorbance curves for NO_3^--N, NO_2^--N, NH_4^+-N, and NH_2OH-N respectively, while (b), (d), (f), and (h) represent the standard curves for NO_3^--N, NO_2^--N, NH_4^+-N, and NH_2OH-N respectively. All of the calibration curves exhibit good linearity.
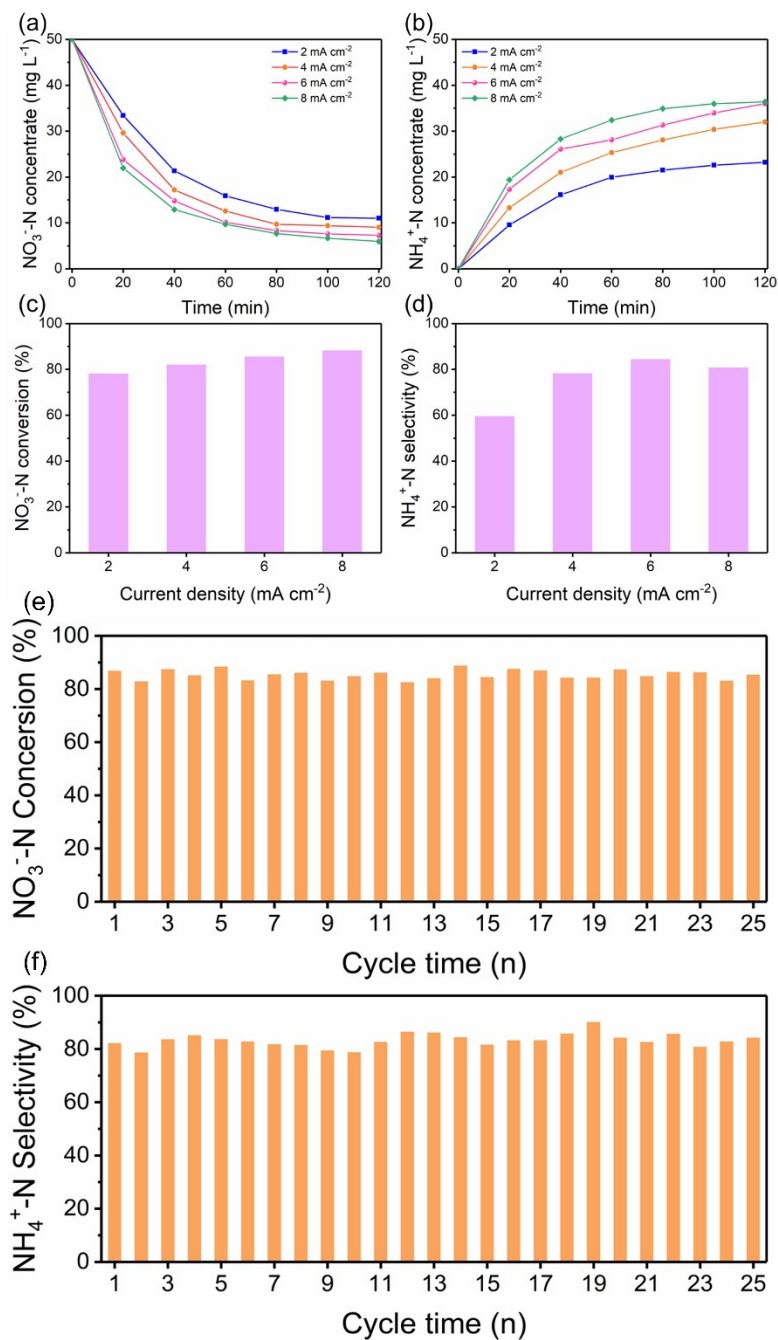
Fig. S16. FeOOH prepared on a self-supporting Ti mesh (10*10 cm). (a)The curve of NO_3^--N concentration versus times under different current densities; (b) The curve of NH_4^+-N concentration versus times under different current densities; (c) The conversion of NO_3^--N and (d) the selectivity of NH_4^+-N under different current densities,
(e) The conversion of NO_3^--N and (f) the selectivity of NH_4^+-N after continuous cycle test.
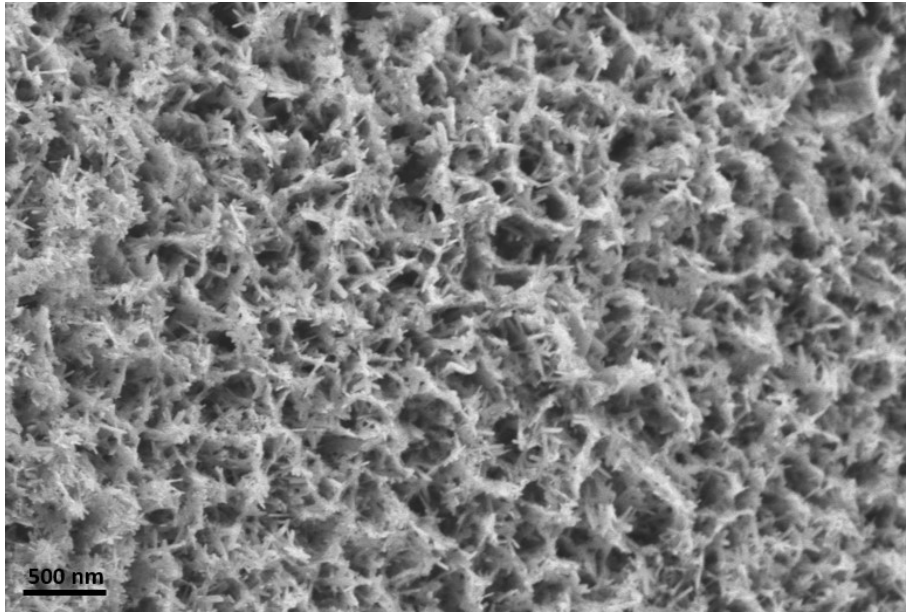
Fig. S17. The SEM image after the electrolysis of NH$_2$OH using FeOOH as the electrode.
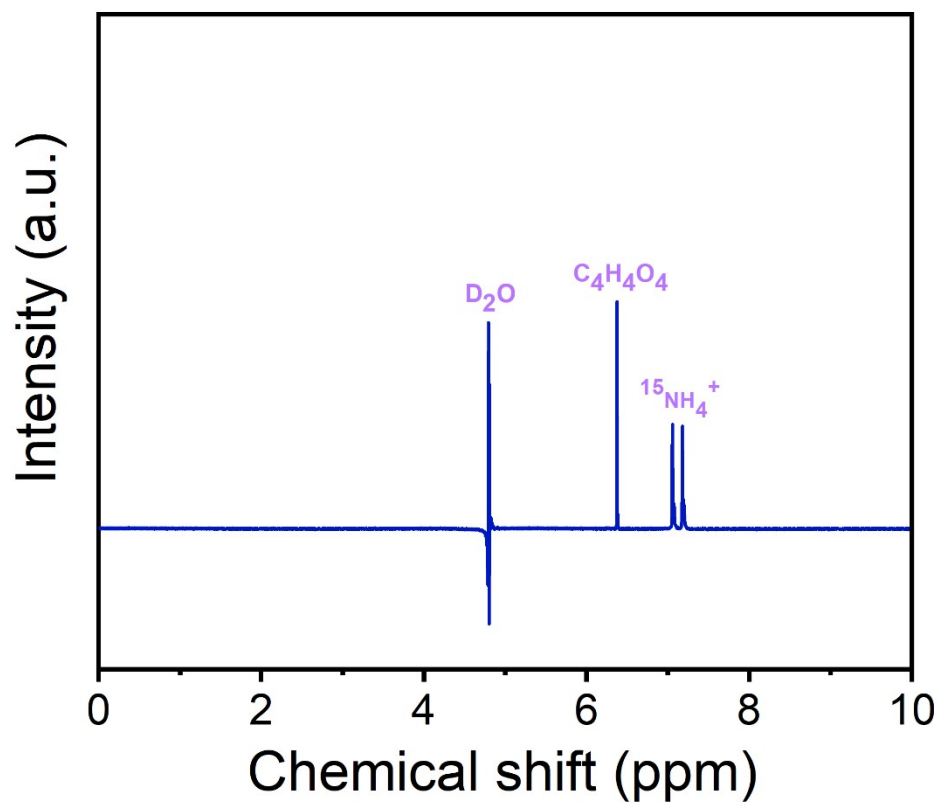
Fig. S18. After 5 cycles, the electrolyte was subjected to nuclear magnetic resonance (NMR) hydrogen spectroscopy testing.
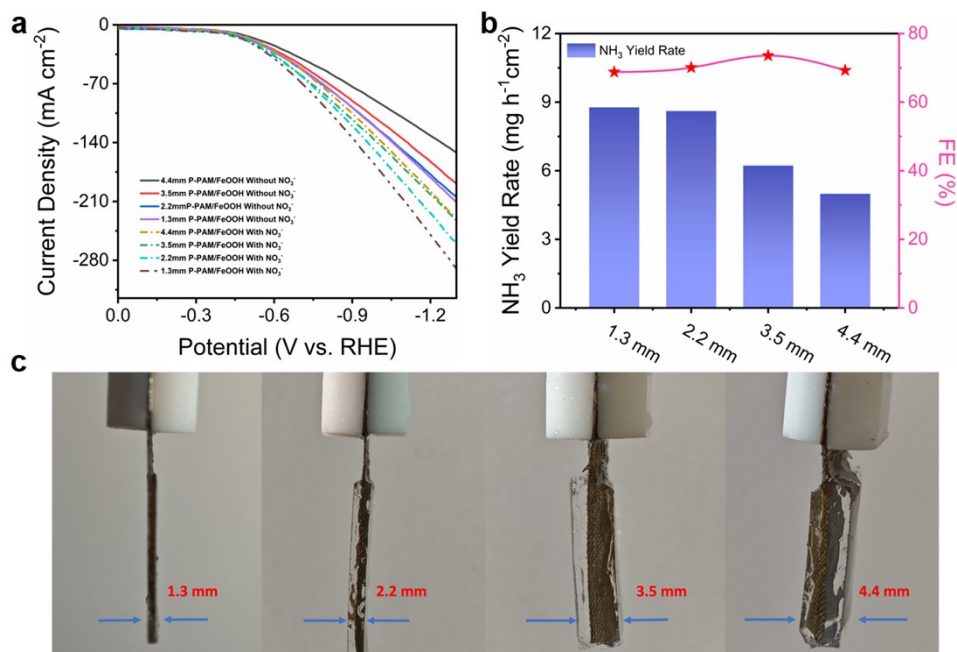
Fig. S19. (a) LSV curves of electrodes loaded with P-PAM of different thicknesses. (b) At -0.8 (V $_{vs}$ RHE), yield and Faradaic Efficiency (FE) of electrodes loaded with P-PAM of different thicknesses. (c) Images of electrodes loaded with P-PAM of different thicknesses.
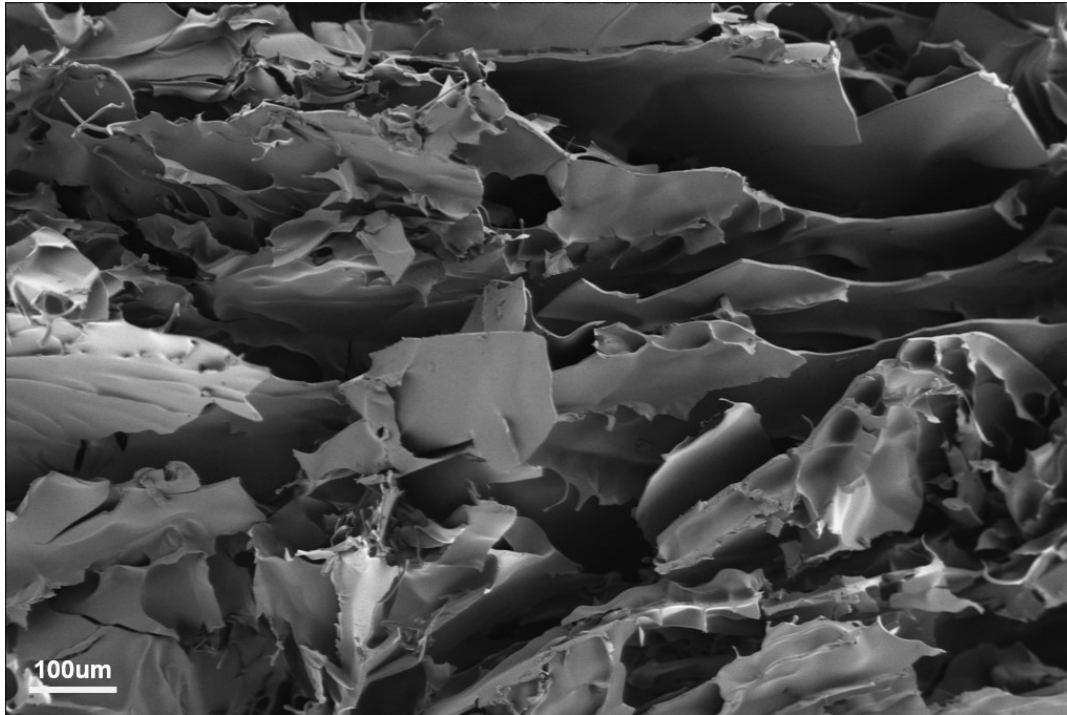
Fig. 20. The internal SEM image of 1.3mm P-PAM hydrogel. Synthesizing P-PAM that is too thin using the ice templating method cannot maintain its internal structure integrity, resulting in poor durability.

Fig. 21. Illustration of the experimental results for the adsorption of NH$_2$OH by P-PAM. The results indicate that after placing the working electrode P-PAM/FeOOH in the NH$_2$OH solution, the concentration of NH$_2$OH in the solution decreased (the lighter the color, the lower the concentration of NH$_2$OH). This demonstrates that P-PAM has an adsorption effect on NH$_2$OH.

Material	Ammonia yield rate ($mg\ h^{-1}\ cm^{-2}$)	Selectivity (%)	Stability. (h)	Whether experiment be scaled up ?	Scaled-up experiment ammonia yield.
Pd-CoOx	30.3	91.3	10	No	
Cl-Cu[1]	0.789	83	20	No	
CR-Cu[2]	3.892	92.8	12	No	
Cu_{SA} NPC[3]	0.26	94.1	10	No	
Co_3O_4GNR[4]	42.11	100	3	No	
Cu_xNi_y/CN[5]	1.755	92.4	7	No	
xP-AC[6]	3.7	90.2	30	No	
$Ni(OH)_2$[7]	0.179	95.5	168	Yes	8.95 $mg\ h^{-1}\ cm^{-2}$
This Work	8.64	89.45	40	Yes	5.74g kWh^{-1}

Table. 1. The performance of different materials used for nitrate reduction in recent studies.

Notes and references

1   B. Zhou; G. M. Zhan; Y. C. Yao; W. X. Zhang; S. X. Zhao; F. J. Quan; C. Y. Fang; Y. B. Shi; Y. Huang; F. L. Jia; L. Z. Zhang, *Water Research* 2023, **242**.

2   Z. Wang; N. Zhou; J. Z. Wang; D. P. Wang; J. R. Zeng; H. X. Zhong; X. B. Zhang, *Chemsuschem* 2024, **17**.

3   X. Y. Zhao; Q. Geng; F. Dong; K. Zhao; S. Chen; H. T. Yu; X. Quan, *Chemical Engineering Journal* 2023, **466**.

4   M. K. R. Souza; E. S. F. Cardoso; L. M. C. Pinto; I. S. C. Crivelli; C. D. Rodrigues; R. S. Souto; A. T. Rezende; M. R. V. Lanza; G. Maia, *Acs Applied Materials & Interfaces* 2024, **17**, 1295-1310.

5   F. Gong; S. H. Hong; J. M. Song; C. Z. Liu; S. L. Liu; J. J. Feng; Q. W. Wu; Y. L. Xiong; L. Medic-Pejic; Y. Cheng; Z. Q. Zhang, *J. Mater. Chem. A* 2024.

6   H. Jung; J. Yang; J. Maeng; W. B. Kim; Y. Yun, *Applied Surface Science* 2025, **686**.

7   W. X. Zheng; L. Y. Zhu; Z. Yan; Z. C. Lin; Z. C. Lei; Y. F. Zhang; H. L. Xu; Z. Dang; C. H. Wei; C. H. Feng, *Environ. Sci. Technol.* 2021, **55**, 13231-13243.